

# Inhibitive Properties, Thermodynamic Characterization and Quantum Chemical Studies of Secnidazole on Mild Steel Corrosion in Acidic Medium

Eno E. Ebenso<sup>1,\*</sup>, Ime B. Obot<sup>2</sup>

<sup>1</sup> Department of Chemistry, North West University (Mafikeng Campus), Private Bag X2046, Mmabatho 2735, South Africa

<sup>2</sup> Department of Chemistry, University of Uyo, PMB 1017, Uyo, Nigeria.

\*E-mail: [Eno.Ebenso@nwu.ac.za](mailto:Eno.Ebenso@nwu.ac.za)

*Received:* 14 October 2010 / *Accepted:* 30 October 2010 / *Published:* 1 December 2010

---

The inhibition of secnidazole (SEC) on the corrosion of mild steel in 0.01-0.04 M H<sub>2</sub>SO<sub>4</sub> at 303-323 K was studied by gravimetric method. Results obtained show that SEC acts as inhibitor for mild steel in H<sub>2</sub>SO<sub>4</sub> solution. The inhibition efficiency was found to increase with increase in SEC concentration but decreased with acid concentration and temperature, which is suggestive of physical adsorption mechanism although chemisorption may play a part. The adsorption of SEC onto the mild steel surface was found to follow the Langmuir adsorption isotherm. Both kinetic parameters (activation energy, pre-exponential factor, enthalpy of activation and entropy of activation) and thermodynamics of adsorption (enthalpy of adsorption, entropy of adsorption and Gibbs free energy) were calculated and discussed. Quantum chemical calculations using DFT at the B3LYP/6-31G\* level of theory was further used to calculate some electronic properties of the molecule in order to ascertain any correlation between the inhibitive effect and molecular structure of secnidazole.

---

**Keywords:** Secnidazole, mild steel, quantum chemistry, sulphuric acid, thermodynamics

## 1. INTRODUCTION

The corrosion of steel is the most common form of corrosion, especially in acid solutions. It has practical importance, for example in the acid pickling of iron and steel, chemical cleaning of the scale in metallurgy, oil recovery and petrochemical industry and other electrochemical systems. During chemical processes, metals suffer from corrosion in acid solutions at elevated temperatures. Corrosion damage is extremely increased when the acid anions form with the metal cation very soluble salt [1]. Generally, increased corrosion-resistance can only be obtained at increased cost. However, the actual material-related costs incurred in a project will depend on the corrosivity of the environment

concerned, the required design life, the physical requirements of the material, and the readily available stocks [2]. In some cases, appearance may also dictate the use of more expensive materials. The costs and problems associated with corrosion-resistance materials means that, in many cases, the use of corrosion inhibitors is a practical and economic alternative.

Most well known acid inhibitors are organic compounds containing nitrogen, sulphur, and oxygen atoms. It is generally accepted that organic molecules inhibit corrosion by adsorption on metal surface. Furthermore, the adsorption depends on the electronic structure of inhibiting molecules, steric factor, aromaticity and electron density at donor site, presence of functional group such as  $-CHO$ ,  $-N=N$ ,  $R-OH$ , etc., molecular area, molecular weight of the molecule, temperature and electrochemical potential at the metal/solution interface [3-10]. Though many organic compounds show good anticorrosive activity, most of them are highly toxic. These inhibitors may cause reversible (temporary) or irreversible (permanent) damage to organ system, namely kidneys or liver, or to disturb a biochemical process or to disturb an enzyme system at some site in the body [11]. The investigation of new non-toxic or low-toxic and green corrosion inhibitors is essential to overcome this problem. In the 21st Century, the research in the field of “green” or “eco-friendly” corrosion inhibitors has been addressed toward the goal of using cheap, effective molecules at low or “zero” environmental impact [12].

A series of reports from our laboratory [13-21] as well as those of other authors [22-38] provide considerable evidence that some drugs could function as effective corrosion inhibitors. The molecular and electronic structures of these drugs, with extensive conjugation and presence of polar N, S or O atoms play very important roles in this regard, facilitating their adsorption on the corroding metal surfaces according to some known adsorption isotherms. In continuation of our studies on the corrosion inhibiting efficacies of drugs, the present investigation was undertaken to elucidate the inhibiting effect of  $\alpha,2$ - dimethyl-5-nitro-1H-imidazole-1-ethanol, a nitromidazole antibacterial drug known commercially as Secnidazole, that has been effective in the treatment of dientamoebiasis [39], on the corrosion of mild steel in sulphuric acid solution under varied experimental conditions. The effect of temperature on corrosion and inhibition processes are thoroughly assessed and discussed. Quantum chemical calculations are also employed to provide additional insight into the mechanism of the inhibitory action.

## 2. EXPERIMENTAL METHOD

### 2.1. Material

Test were performed on a freshly prepared sheet of mild steel of the following composition (wt.%): 0.13% C, 0.18% Si, 0.39% Mn, 0.40% P, 0.04% S, 0.025% Cu, and bal Fe. The metal specimens were prepared, degreased and cleaned as previously described [4, 8].

### 2.2. Inhibitor

Secnidazole (SEC) was purchased as Flagentyl (brand name) from May and Baker pharmaceuticals. Stock solution of SEC was made in 10:1 water: methanol mixture to ensure solubility

[38]. This stock solution was used for all experimental purposes. Fig.1 shows the molecular structure of SEC. It is evident that SEC is a heterocyclic compound containing nitrogen and oxygen atoms, which could easily be protonated in acidic solution, and some  $\pi$ -electrons exist in this molecule.

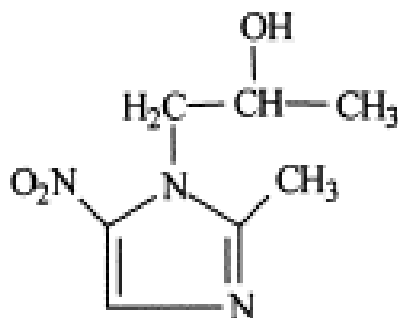


**Figure 1.** Molecular structure of Secnidazole (SEC).

### 2.3. Solutions

The aggressive solutions, 0.01-0.04M  $\text{H}_2\text{SO}_4$  were prepared by dilution of analytical grade 98%  $\text{H}_2\text{SO}_4$  with distilled water. The concentration range of SEC was  $1 \times 10^{-3}$ – $5 \times 10^{-3}$ M.

### 2.4. Gravimetric measurements

The gravimetric method (weight loss) is probably the most widely used method of inhibition assessment [40-46]. The simplicity and reliability of the measurements offered by the weight loss method is such that the technique forms the baseline method of measurement in many corrosion monitoring programmes [2]. Weight loss measurements were conducted under total immersion using 250 mL capacity beakers containing 200 mL test solution at 303-323 K maintained in a thermostated water bath. The mild steel coupons were weighed and suspended in the beaker with the help of rod and hook. The coupons were retrieved at 2 h interval progressively for 10 h, washed thoroughly in 20% NaOH solution containing 200 g/l of zinc dust [15] with bristle brush, rinsed severally in deionized water, cleaned, dried in acetone, and re-weighed. The weight loss, in grammes, was taken as the difference in the weight of the mild steel coupons before and after immersion in different test solutions. Then the tests were repeated at different temperatures. In order to get good reproducibility, experiments were carried out in triplicate. In this present study, the standard deviation values among parallel triplicate experiments were found to be smaller than 5%, indicating good reproducibility.

The corrosion rate ( $\rho$ ) in  $\text{g cm}^{-2} \text{h}^{-1}$  was calculated from the following equation [41]:

$$\rho = \frac{\Delta W}{St} \quad (1)$$

where  $W$  is the average weight loss of three mild steel sheets,  $S$  the total area of one mild steel specimen, and  $t$  is the immersion time (10 h). With the calculated corrosion rate, the inhibition efficiency (%I) was calculated as follows [42]:

$$\%I = \left( \frac{\rho_1 - \rho_2}{\rho_1} \right) \times 100 \quad (2)$$

Where  $\rho_1$  and  $\rho_2$  are the corrosion rates of the mild steel coupons in the absence and presence of inhibitor, respectively.

### 2.5. Computational details

B3LYP, a version of the DFT method that uses Becke's three-parameter functional (B3) and includes a mixture of HF with DFT exchange terms associated with the gradient corrected correlation functional of Lee, Yang, and Parr (LYP) has been recognized especially for systems containing transition metal atoms [6]. It has much less convergence problems than those commonly found for pure DFT methods. Thus, B3LYP was used in this work to carry out quantum calculations. Then, full geometry optimization of the inhibitor was carried out at the B3LYP/6-31G\* level using the Spartan'06 V112 program package.

## 3. RESULTS AND DISCUSSION

### 3.1. Effect of SEC on corrosion rate

A number of mechanistic studies on the anodic dissolution of Fe in acidic sulphate solutions have been undertaken, and the hydroxyl accelerated mechanism proposed initially by Bockris and Drazic [47] has gained overwhelming acceptance.



where 'rds' represents the rate determining step. The Fe electro-dissolution in acidic sulphate solutions depends primarily on the adsorbed intermediate  $\text{FeOH}_{\text{ads}}$ . Consequently, Ashassi-Sorkhabi and Nabavi-Amri [48] proposed the following mechanism involving two adsorbed intermediates in order to account for the retardation of Fe anodic dissolution in the presence of an inhibitor.





where 'rds' denotes the rate determining step and Y represents the inhibitor species.

Considering the inhomogeneous nature of metallic surfaces resulting from the existence of lattice defects and dislocations, a corroding metal surface is generally characterized by multiple adsorption sites having definite activation energies and heat of adsorption. Inhibitor molecules may thus be adsorbed more readily at surface sites having suitable adsorption enthalpies. According to the detailed mechanism above, displacement of some adsorbed water molecules on the metal surface by inhibitor species to yield the adsorbed intermediate  $\text{FeY}_{\text{ads}}$  (Eq. 8) reduces the amount of species  $\text{FeOH}_{\text{ads}}^-$  available for the rate determining step and consequently retards Fe anodic dissolution.

The corrosion rate curves of mild steel with the addition of SEC in 0.01 M  $\text{H}_2\text{SO}_4$  at 303-323K are shown in Fig. 2.

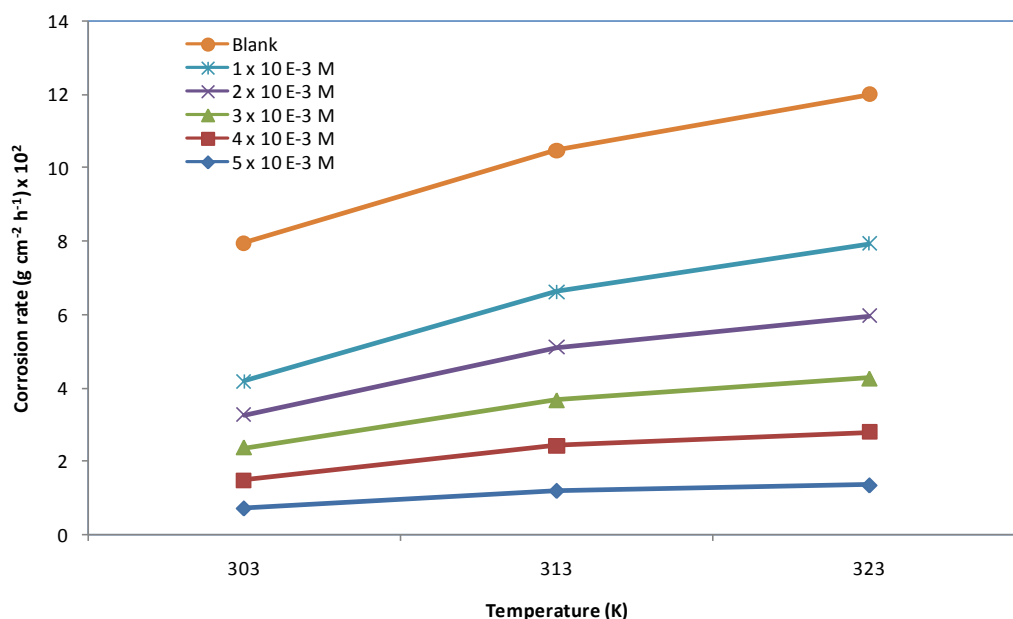


**Figure 2.** Relationship between corrosion rate and temperature for different concentrations of Secnidazole (SEC) in 0.01 M  $\text{H}_2\text{SO}_4$ .

Inspection of the figure reveals that the corrosion rate decreases as the concentrations of inhibitor increases, i.e. the corrosion inhibition enhances with inhibitor concentration. This behaviour is due to the fact that the amount of coverage of SEC on mild steel surface increases with inhibitors concentration [49]. Thus, the mild steel surface is efficiently separated from the acid medium [50, 51]. Also the curves in Fig. 2 show that the corrosion rate of mild steel increases with increasing temperature both in uninhibited and inhibited solution. However, the corrosion rate increases more rapidly with temperature in the absence of inhibitor. These results confirm that SEC acts as an efficient inhibitor in the range of studied temperature.

### 3.2. Inhibition efficiency dependence on concentration of SEC and temperature

The plot of inhibition efficiencies obtained from weight loss for different inhibitor concentrations in 0.01 M H<sub>2</sub>SO<sub>4</sub> is shown in Fig. 3.

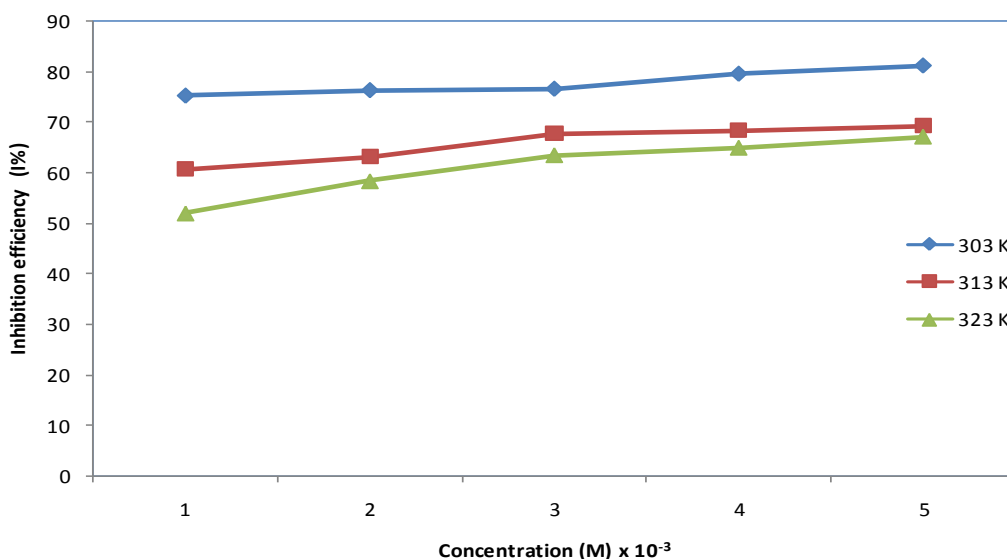


**Figure 3.** Relationship between inhibition efficiency and concentration of Secnidazole (SEC) at different temperatures in 0.01 M H<sub>2</sub>SO<sub>4</sub>.

It is evident from the figure that inhibition efficiency (%*I*) increases as the concentration of inhibitor increases from 1 x 10<sup>-3</sup> to 5 x 10<sup>-3</sup> M. The optimum concentration for maximum efficiency was found to be 5 x 10<sup>-3</sup> M. At the optimum concentration, the efficiency attains 81.2% at 303 K. The inhibition efficiency was found to be 75.4% at 303 K even at the lowest concentration studied (1 x 10<sup>-3</sup> M). Such remarkable performances may be due to the high molecular weight of SEC, the presence of C=N, R-OH which are electron rich centres and π -electrons of the imidazole moiety. A further increase of inhibitor concentration does not significantly change the protective effect. Fig. 3 also shows that %*I* decreases with experimental temperature, which can be attributed to the fact that the higher temperatures might cause desorption of SEC from the steel surface [49]. This can be due to the

decrease in the strength of adsorption process at higher temperatures, suggesting that physical adsorption may be the type of adsorption of the inhibitor on the sample surfaces [52, 53].

### 3.3. Effect of sulphuric acid concentration on corrosion inhibition

The effect of sulphuric acid concentration (0.01-0.04 M) on corrosion inhibition of mild steel was also studied in order to get general information of the corrosion inhibition of SEC.

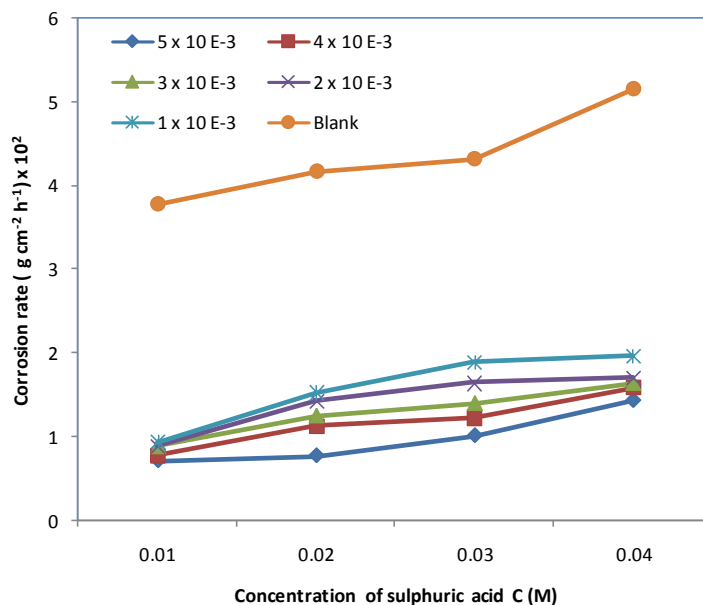


Figure 4. The relationship between corrosion rate and the concentration of H<sub>2</sub>SO<sub>4</sub> at 303K

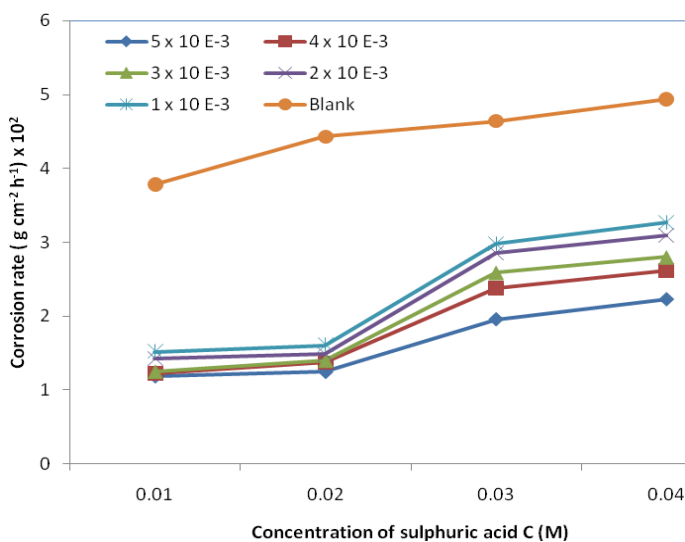


Figure 5. The relationship between corrosion rate and the concentration of H<sub>2</sub>SO<sub>4</sub> at 313K.

Figs. 4-6 show the relationship between corrosion rate ( $\rho$ ) and sulphuric acid concentration (M) at 303-323 K (immersion time 10 h). From the plots, the corrosion rate is observed to increase with increase in  $H_2SO_4$  concentrations both in the absence and presence of SEC. However, in the presence of SEC, the corrosion rate decreased with increase of SEC in the whole  $H_2SO_4$  concentration studied.

### 3.4. Rate constant and reaction constant

Mathur and Vasudevan [54] proposed that a linear relationship exist between the corrosion rate and the molar concentration of acid solution given by the equation:

$$\ln v = \ln k + BC \tag{13}$$

Where  $k$  is the rate constant,  $B$  the reaction constant, and  $C$  is the molar concentration of  $H_2SO_4$ . Fig. 7 shows the relationship between  $\ln v$  and sulphuric acid concentrations ( $C$ ) at different conditions. It is evident from Fig. 7 that there is a good linear relationship between  $\ln v$  and  $C$ .

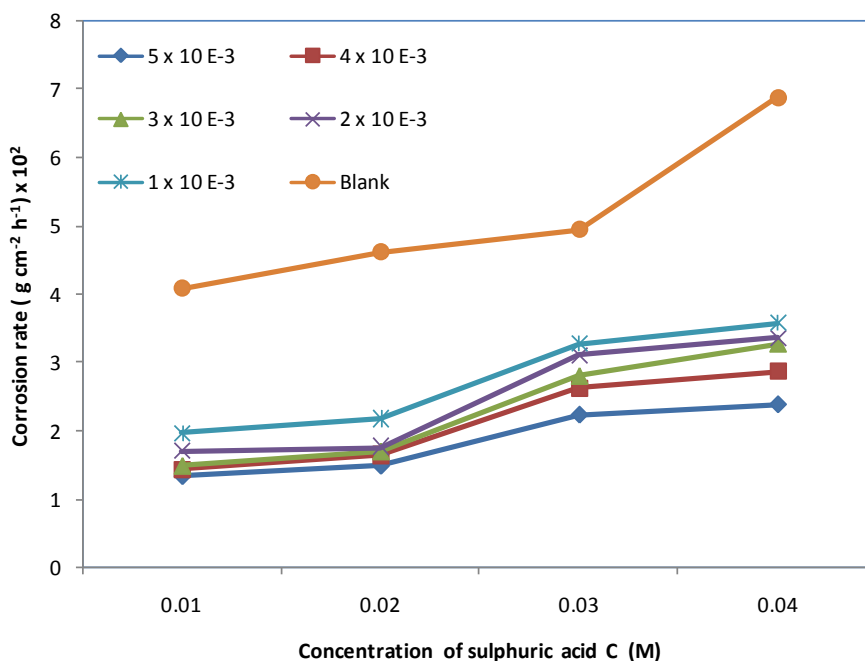


**Figure 6.** The relationship between corrosion rate and the concentration of  $H_2SO_4$  at 303K.

The straight lines obtained are an indication to the fit of equation (13) to the experimental data. The kinetic parameters obtained from equation (13) are listed in Table 1. The linear regression coefficients ( $r$ ) listed in Table 1 are very close to 1, which also indicates a strong dependence of  $\ln v$  on  $C$ .

**Table 1.** Parameters of the linear regression between  $\ln v$  and  $C$  for the corrosion of steel in  $H_2SO_4$  containing SEC at 303 K

C (M)	Linear Regression (r)	$k$ ( $g\ cm^{-2}h^{-1}$ )	$B$ ( $g\ cm^{-2}h^{-1}M^{-1}$ )
Blank	0.931	$3.38 \times 10^2$	0.097
$1 \times 10^{-3}$	0.900	$8.16 \times 10^1$	0.245
$2 \times 10^{-3}$	0.920	$8.15 \times 10^1$	0.207
$3 \times 10^{-3}$	0.933	$7.62 \times 10^1$	0.200
$4 \times 10^{-3}$	0.946	$6.45 \times 10^1$	0.225
$5 \times 10^{-3}$	0.938	$5.18 \times 10^1$	0.238

The value of  $k$  denotes the ability of corrosion of  $H_2SO_4$  for mild steel [54, 55]. Table 1 clearly shows that  $k$  decreases after addition of SEC to  $H_2SO_4$  solution, and follows the order:  $k ( 5 \times 10^{-3} M) < k ( 4 \times 10^{-3} M) < k ( 3 \times 10^{-3} M) < k ( 2 \times 10^{-3} M) < k ( 1 \times 10^{-3} M)$ , which indicates that the corrosion of mild steel is drastically inhibited by the SEC inhibitor.  $B$  is the slope of the line according to equation (13) and it indicates the extent of change of corrosion rate with acid concentration [49]. The values of  $B$  obtained in inhibited sulphuric acid solution is higher than in uninhibited sulphuric acid solution, which indicates that the extent of change of  $v$  with  $C$  in inhibited  $H_2SO_4$  is higher than in uninhibited  $H_2SO_4$ .

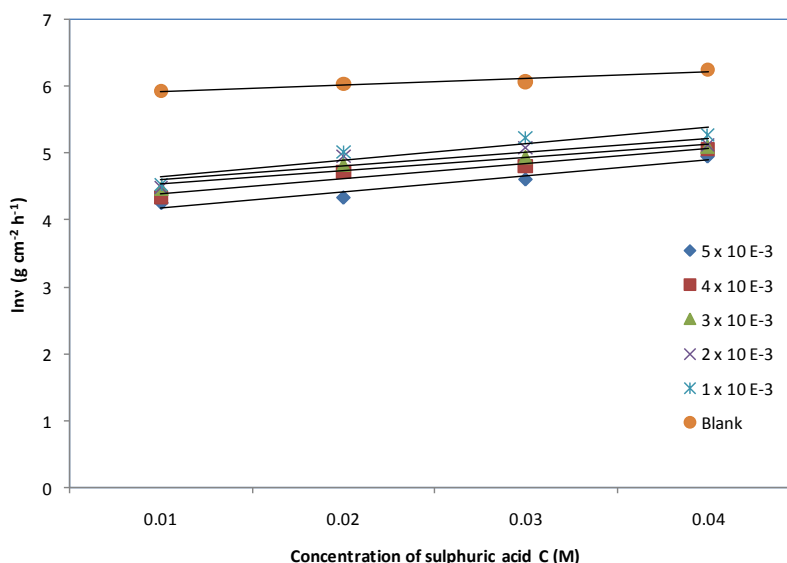


**Figure 7.** The relationship between  $\ln v$  and concentration of  $H_2SO_4$  at 303K

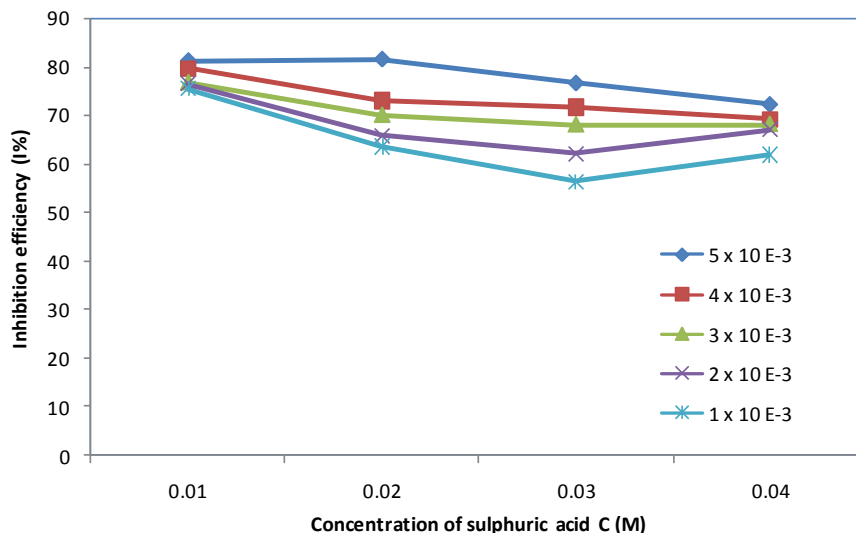


**Figure 8.** The relationship between inhibition efficiency (I%) at different concentrations of Secnidazole (SEC) and the concentration of H<sub>2</sub>SO<sub>4</sub> at 303K.

3.5. Effect of Changing H<sub>2</sub>SO<sub>4</sub> concentration on the inhibition efficiency

Fig. 8 shows the effect of changing H<sub>2</sub>SO<sub>4</sub> concentration (0.01-0.04 M) at 303 K on the inhibition efficiency of SEC at different concentrations studied. In all cases, increasing acid concentration resulted in decreasing inhibition efficiency. However, inhibition efficiency was found to increase with increase in the concentration of SEC at the range of acid concentration studied (0.01-0.04 M). Such behaviour may be considered in line with the suggestion that the adsorption mechanism for a given inhibitor depends on the concentration of inhibitor [56-58].

3.6. Effect of Temperature and activation parameters on the inhibition process

Temperature plays an important role in understanding the inhibitive mechanism of the corrosion process. To assess the effect of temperature on corrosion and corrosion inhibitive process, weight loss experiments were performed at 10 K intervals in the temperature range 303-323 K in uninhibited acid (0.01M H<sub>2</sub>SO<sub>4</sub>) and in inhibited solutions containing different concentrations of SEC. The results obtained for a 10 h immersion period is given in Fig. 2 and shows that corrosion rates in both uninhibited and inhibited acid increased with rise in temperature. The relationship between the corrosion rate ( $\rho$ ) of mild steel in acidic media and temperature ( $T$ ) is often expressed by the Arrhenius equation [40, 41]:

$$\log \rho = \log A - \frac{E_a}{2.303RT} \tag{14}$$

where  $\rho$  is the corrosion rate,  $E_a$  is the apparent activation energy,  $R$  is the molar gas constant (8.314 J K<sup>-1</sup> mol<sup>-1</sup>),  $T$  is the absolute temperature, and  $A$  is the frequency factor. The plot of  $\log \rho$

against  $1/T$  for mild steel corrosion in 0.01 M  $H_2SO_4$  in the absence and presence of different concentrations of SEC is presented in Fig. 9.

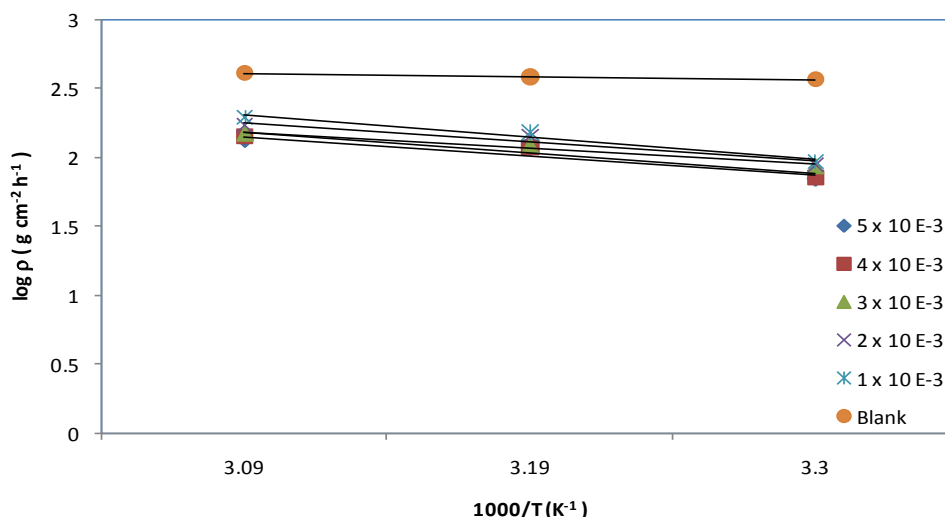


**Figure 9.** Arrhenius plot for mild steel corrosion in 0.01 M  $H_2SO_4$  in the absence and presence of different concentrations of Secnidazole (SEC).

All parameters are given in Table 2.

**Table 2.** Activation parameters of the dissolution of mild steel in 0.01 M  $H_2SO_4$  in the absence and presence of different concentrations of SEC.

C (M)	A (g cm <sup>-2</sup> h <sup>-1</sup> )	E <sub>a</sub> (kJ mol <sup>-1</sup> )	ΔH* (kJ mol <sup>-1</sup> )	ΔS* (J mol <sup>-1</sup> K <sup>-1</sup> )
Blank	1.56 x 10 <sup>3</sup>	3.618	1.921	-194.32
1 x 10 <sup>-3</sup>	1.15 x 10 <sup>6</sup>	29.46	27.20	-117.33
2 x 10 <sup>-3</sup>	2.49 x 10 <sup>6</sup>	25.69	23.32	-130.41
3 x 10 <sup>-3</sup>	4.20 x 10 <sup>5</sup>	21.31	19.32	-147.13
4 x 10 <sup>-3</sup>	3.53 x 10 <sup>6</sup>	27.07	25.13	-135.50
5 x 10 <sup>-3</sup>	1.83 x 10 <sup>6</sup>	25.46	23.84	-133.74

From Table 2, it is evident that the value of  $E_a$  in the presence of SEC is higher than that in the uninhibited acid solution. According to equation (14), it is clear that the lower  $A$  and the higher  $E_a$  lead to the lower corrosion rate ( $\rho$ ). For the present study, the value of  $A$  in the presence of SEC is higher than that in uninhibited solution and so the decrease in steel corrosion rate is determined by the

apparent activation energy ( $E_a$ ). Similar report has been documented previously [49]. The relationships between the temperature dependence of %I of an inhibitor and the  $E_a$  can be classified into three groups according to temperature effects [59];

1. %I decreases with increase in temperature,  $E_a$  (inhibited solution) >  $E_a$  (uninhibited solution).
2. %I increases with increase in temperature,  $E_a$  (inhibited solution) <  $E_a$  (uninhibited solution).
3. %I does not change with temperature,  $E_a$  (inhibited solution) =  $E_a$  (uninhibited solution).

It is clear from Table 2, that case (i) is applicable in this work, i.e.  $E_a$  in the inhibited solution is higher than that obtained for the free acid solution indicating that the corrosion reaction of mild steel is inhibited by SEC [60], hence supports the phenomenon of physical adsorption [6-8]. Higher values of  $E_a$  in the presence of inhibitor can be correlated with increasing thickness of the double layer which enhances the  $E_a$  of the corrosion process [41]. It is also an indication of a strong inhibitive action of SEC by increasing energy barrier for the corrosion process, emphasizing the electrostatic character of the inhibitor’s adsorption on the mild steel surface (physisorption) [40].

Experimental corrosion rate values obtained from weight loss measurements for mild in 0.01 M  $H_2SO_4$  in the absence and presence of SEC was used to further gain insight on the change of enthalpy ( $\Delta H^*$ ) and entropy ( $\Delta S^*$ ) of activation for the formation of the activation complex in the transition state using transition equation [61]:

$$\rho = \left(\frac{RT}{Nh}\right) \exp\left(\frac{\Delta S^*}{R}\right) \exp\left(\frac{-\Delta H^*}{RT}\right) \tag{15}$$

where  $\rho$  is the corrosion rate,  $h$  is the Planck’s constant ( $6.626176 \times 10^{-34}$  Js),  $N$  is the Avogadro’s number ( $6.02252 \times 10^{23}$  mol<sup>-1</sup>),  $R$  is the universal gas constant and  $T$  is the absolute temperature. Fig. 10 shows the plot of  $\log \rho/T$  versus  $1/T$  for mild steel corrosion in 0.01 M  $H_2SO_4$  in the absence and presence of different concentrations of SEC.

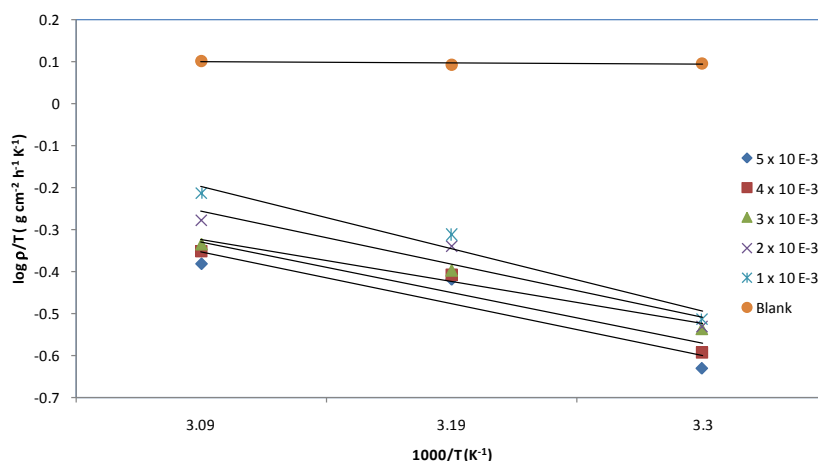


**Figure 10.** Transition state plot for mild steel corrosion in 0.01 M  $H_2SO_4$  in the absence and presence of different concentrations of Secnidazole (SEC).

Straight lines were obtained with slope of  $(\Delta H^*/2.303R)$  and an intercept of  $[\log(R/Nh) + (\Delta S^*/2.303R)]$  from which the values of  $\Delta H^*$  and  $\Delta S^*$  respectively were computed and listed also in Table 2. The positive values of  $\Delta H^*$  both in the absence and presence of SEC reflect the endothermic nature of the steel dissolution process. From Table 2, it is seen that the value of activation energy and enthalpy of activation varied in the same way. This result verified the known thermodynamic relation between  $E_a$  and  $\Delta H^*$  [62, 63]:

$$\Delta H^* = E_a - RT \quad (16)$$

The values of enthalpy of activation calculated from graphical and mathematical models using Eqs. (15) and (16) are almost the same confirming the above relation. The negative values of entropy of activation both in the absence and presence of inhibitor imply that the activated complex in the rate determining step represents an association rather than a dissociation step, meaning that a decrease in disordering takes place on going from reactants to the activated complex [64, 65].

### 3.7. Adsorption isotherm and thermodynamic consideration

Corrosion inhibition by organic compounds is mainly due to their ability to adsorb onto a metal surface to form a protective film. The establishment of isotherms that describe the adsorption behaviour of corrosion inhibitor is important as they provide clues about the nature of metal-inhibitor interaction. A direct relationship between inhibition efficiency ( $\%I$ ) and the degree of surface coverage ( $\theta$ ) [ $\%I = 100 \times \theta$ ] can be assumed for the different concentration of the inhibitor. The degree of surface coverage ( $\theta$ ) for the different concentrations of SEC has been evaluated from the weight loss measurements in 0.01 M  $H_2SO_4$  at 303-323 K for 10 h of immersion period. The data were graphically fitted to various adsorption isotherms including Freundlich, Temkin, Flory-Huggins, Bockris-Swinkles, Langmuir and Frumkin isotherms. The correlation coefficient ( $r$ ) was used to determine the best fit isotherm which was obtained for Langmuir. According to this isotherm,  $\theta$  is related to the inhibitor concentration by the following equation [66]:

$$\frac{C}{\theta} = \frac{1}{K_{ads}} + C \quad (17)$$

where  $\theta$  is the degree of surface coverage,  $C$  is the concentration,  $K_{ads}$  is the equilibrium constant of adsorption process.  $K_{ads}$  is related to the free energy of adsorption  $\Delta G_{ads}^o$  by the equation [67]:

$$\log K_{ads} = -\log C_{H_2O} - \frac{\Delta G_{ads}^o}{2.303RT} \quad (18)$$

where  $C_{H_2O}$  is the concentration of water expressed in mol/L (the same as that of inhibitor concentration),  $R$  is the molar gas constant ( $\text{kJ mol}^{-1}\text{K}^{-1}$ ) and  $T$  is the absolute temperature ( $K$ ).

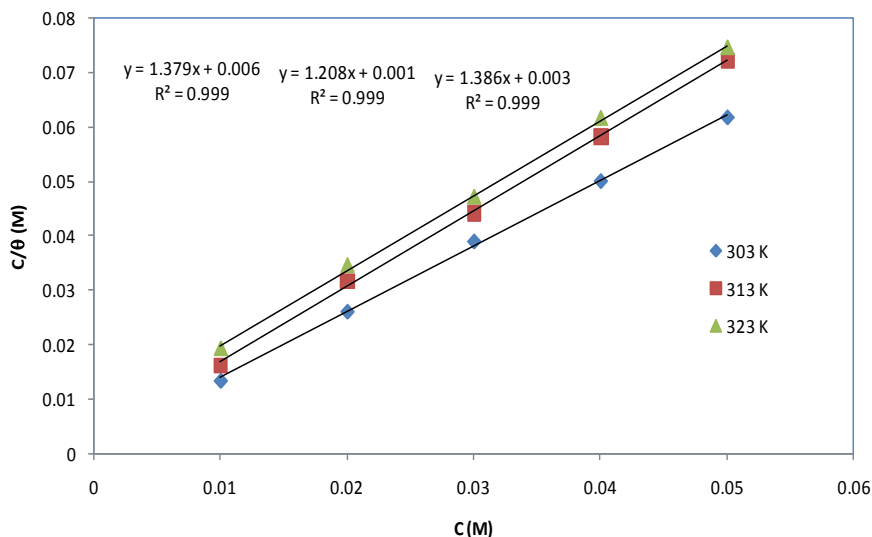


**Figure 11.** Langmuir adsorption model for mild steel in 0.01 M  $H_2SO_4$  containing Secnidazole (SEC) at different temperatures.

Fig. 11 shows that the plot of  $C/\theta$  vs.  $C$  and linear plots were obtained for the different temperatures indicating that the adsorption of SEC followed Langmuir isotherm. The various adsorption parameters obtained from this isotherm are listed in Table 3.

**Table 3.** Some parameters from Langmuir isotherm model for mild steel in 0.01 M  $H_2SO_4$ .

Temperature (K)	slope	$K_{ads}$ (M)	(r)	$\Delta G^o_{ads}$ ( $\text{kJ mol}^{-1}$ )
303	1.21	$1.0 \times 10^3$	0.999	-27.52
313	1.38	$3.3 \times 10^2$	0.999	-25.54
323	1.37	$1.6 \times 10^2$	0.999	-24.41

It is seen from the table that the correlation coefficients are very good and  $K_{ads}$  values decrease with an increase in temperature. Large values of  $K_{ads}$  mean better inhibition efficiency of the inhibitor, i.e., strong electrical interaction between the double-layer existing at the phase boundary and the adsorbing inhibitor molecules. Small values of  $K_{ads}$ , however, reveal that such interactions between adsorbing inhibitor molecules and the metal surface are weaker, indicating that the inhibitor molecules are easily removable by the solvent molecules from the metal surface [68]. These results confirm the suggestion that SEC is physically adsorbed on the metal surface and that the strength of the adsorption

decreases with temperature. Although Langmuir plots are linear as depicted by  $r$  values (0.999), however, the slopes deviates slightly from the value of unity as expected from ideal Langmuir adsorption equation. This deviation may be explained on the basis of interaction among adsorbed species on the surface of the metal. It has been postulated in the deviation of Langmuir isotherm equation that adsorbed molecules do not interact with one another, but this is not true in the case of large organic molecules (such as SEC) having polar atoms or groups which can adsorb on the cathodic and anodic sites of the metal surface. Such adsorbed species interact by mutual repulsion or attraction. It is also possible that the inhibitor studied can adsorb on the anodic and cathodic sites resulting in deviation from unit gradient. Similar observation has been documented by Solomon et al. [41] and other authors [69, 70].

Calculated free energies  $\Delta G_{ads}^o$  values are given also in Table 3. The negative values of  $\Delta G_{ads}^o$  indicate spontaneous adsorption of SEC onto the mild steel surface [71] and strong interactions between inhibitor molecules and the metal surface [72].

Generally, values of  $\Delta G_{ads}^o$  up to  $-20 \text{ kJ mol}^{-1}$  are consistent with physisorption, while those around  $-40 \text{ kJ mol}^{-1}$  or higher are associated with chemisorption as a result of the sharing or transfer of electrons from organic molecules to the metal surface to form a coordinate bond [73].

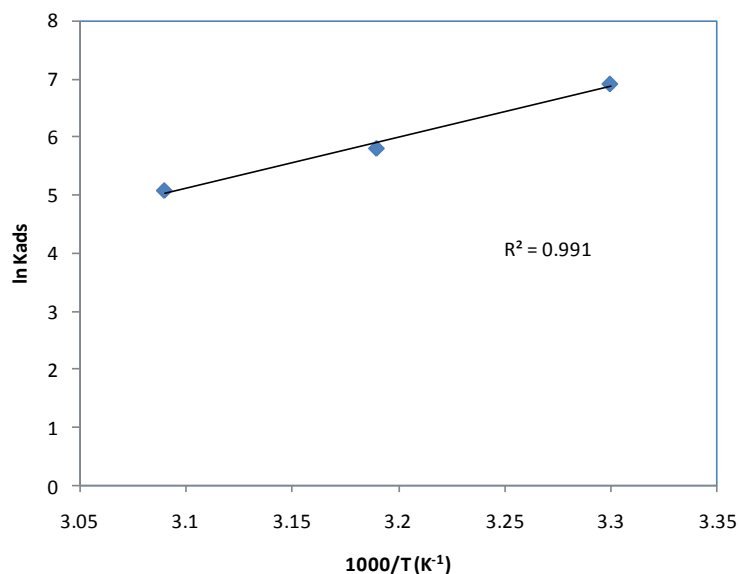


**Figure 12.** The relationship between  $\ln K_{ads}$  and  $1/T$

The calculated values of  $\Delta G_{ads}^o$  are greater than  $-20 \text{ kJ mol}^{-1}$  but less than  $-40 \text{ kJ mol}^{-1}$ , indicating that the adsorption mechanism of SEC on mild steel in  $0.01 \text{ M H}_2\text{SO}_4$  solution at the studied temperatures may be a combination of both physisorption and chemisorption (comprehensive adsorption) [74]. However, physisorption was the major contributor while chemisorption only slightly contributed to the adsorption mechanism judging from the decrease of  $\%I$  with increase in temperature and the higher values of  $E_a$  obtained in the presence of inhibitor when compared to its absence.

Thermodynamic parameters such as enthalpy of adsorption  $\Delta H_{ads}^o$  and entropy of adsorption  $\Delta S_{ads}^o$  can be deduced from integrated version of the van't Hoff equation expressed by [75]:

$$\ln K_{ads} = -\frac{\Delta H_{ads}^o}{RT} + \frac{\Delta S_{ads}^o}{R} + \ln \frac{1}{55.5} \tag{19}$$

Fig. 12 shows the plot of  $\ln K_{ads}$  versus  $1/T$  which gives straight lines with slope of  $(-\Delta H_{ads}^o/R)$  and intercepts of  $(\Delta S_{ads}^o/R + \ln 1/55.5)$ . Calculated value of  $\Delta H_{ads}^o$  and  $\Delta S_{ads}^o$  using the van't Hoff equation are  $-72.71 \text{ kJ mol}^{-1}$  and  $-149.70 \text{ J mol}^{-1} \text{ K}^{-1}$  respectively.

The enthalpy of adsorption can also be calculated from the Gibbs-Helmholtz equation [76]:

$$\left[ \frac{\partial(\Delta G_{ads}^o/T)}{\partial T} \right]_p = -\frac{\Delta H_{ads}^o}{T^2} \tag{20}$$

Equation (20) can be arranged to give the following equation:

$$\frac{\Delta G_{ads}^o}{T} = \frac{\Delta H_{ads}^o}{T} + k \tag{21}$$

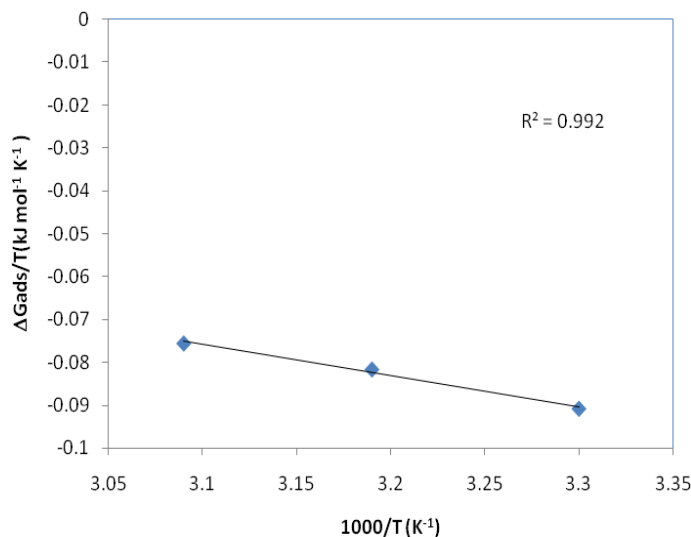


**Figure 13.** The relationship between  $\Delta G_{ads}^o/T$  and  $1/T$

The variation of  $\Delta G_{ads}^o/T$  with  $1/T$  gives a straight line with a slope equal to  $\Delta H_{ads}^o$  (Fig.13). It can be seen from the figure that  $\Delta G_{ads}^o/T$  decreases with  $1/T$  in a linear fashion. The obtained value of  $\Delta H_{ads}^o$  ( $-70.00 \text{ kJ mol}^{-1}$ ) agrees with the one obtained using van't Hoff equation.

The enthalpy and entropy for the adsorption of SEC on mild steel were also deduced from the thermodynamic basic equation [77]:

$$\Delta G_{ads}^{\circ} = \Delta H_{ads}^{\circ} - T\Delta S_{ads}^{\circ} \quad (22)$$

where  $\Delta H_{ads}^{\circ}$  and  $\Delta S_{ads}^{\circ}$  are the enthalpy and entropy changes of adsorption process, respectively. A plot of  $\Delta G_{ads}^{\circ}$  versus T was linear (Fig. 14) with the slope equal to  $-\Delta S_{ads}^{\circ}$  and intercept of  $\Delta H_{ads}^{\circ}$ .

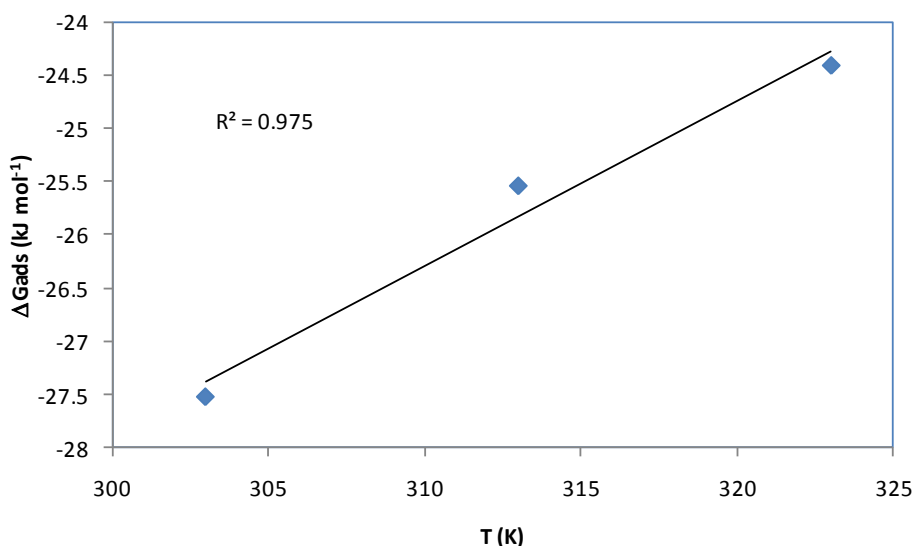


**Figure 14.** The relationship between  $\Delta G_{ads}^{\circ}$  and T

The enthalpy of adsorption  $\Delta H_{ads}^{\circ}$ , and the entropy of adsorption  $\Delta S_{ads}^{\circ}$ , obtained are  $-74.49 \text{ kJ mol}^{-1}$  and  $-155.00 \text{ J mol}^{-1} \text{ K}^{-1}$  respectively. The negative sign of  $\Delta H_{ads}^{\circ}$  indicates that the adsorption of SEC molecules is an exothermic process. In an exothermic process, physisorption is distinguished from chemisorption by considering the absolute value of  $\Delta H_{ads}^{\circ}$ . For physisorption process, the enthalpy of adsorption is lower than  $40 \text{ kJ mol}^{-1}$  while that for chemisorption approaches  $100 \text{ kJ mol}^{-1}$  [78]. In the present case,  $\Delta H_{ads}^{\circ}$  values are larger than the common physical adsorption heat, but smaller than the common chemical adsorption heat, once again emphasizing that both physical and chemical adsorption are involved. Similar results were reported elsewhere [79, 80]. Values of  $\Delta H_{ads}^{\circ}$  obtained by the three methods are in good agreement.

The entropy of adsorption obtained from equations (19) and (22) are large and negative because inhibitor molecule freely moving in the bulk solution (inhibitor molecule were chaotic), were adsorbed in an orderly fashion onto the mild steel, resulting in a decrease in entropy [81]. Moreover, from thermodynamic principles, since the adsorption was an exothermic process, it must be accompanied by a decrease in entropy [82].

### 3.8. Quantum chemical studies

Quantum chemical calculations can complement the experimental investigations or even predict with some confidence into experimentally unknown properties [83, 84]. There has been increasing use of the density functional theory (DFT) methods in applications related to organic and bioorganic compounds [85]. The advancement in methodology and implementations has reached a point where predicted properties of reasonable accuracy can be obtained from DFT calculations [86]. Thus in the present investigation, quantum chemical calculation using DFT was employed to explain the experimental results obtained in this study and to further give insight into the inhibition action of SEC on the mild steel surface.

Figs. 15-19 show the optimized geometry, the HOMO density distribution, the LUMO density distribution, the Mulliken charge population analysis and the total electron density plots for SEC molecule obtained with DFT at B3LYP/6-31G\* level of theory. Table 4 shows the calculated quantum chemical properties for SEC.

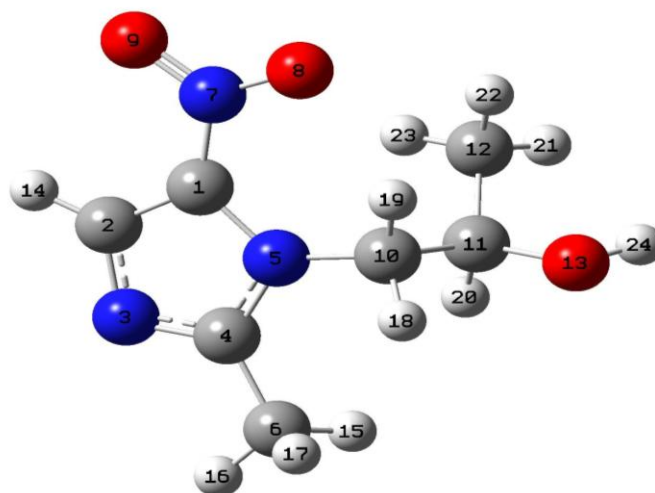


**Figure 15.** Optimized structure of Secnidazole (SEC) (ball and stick model).

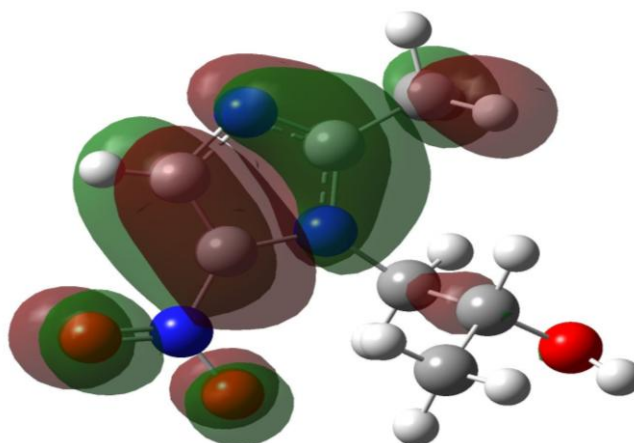


**Figure 16.** The highest occupied molecular orbital (HOMO) density of Secnidazole (SEC) using DFT at the B3LYP/6-31G\* basis set level.

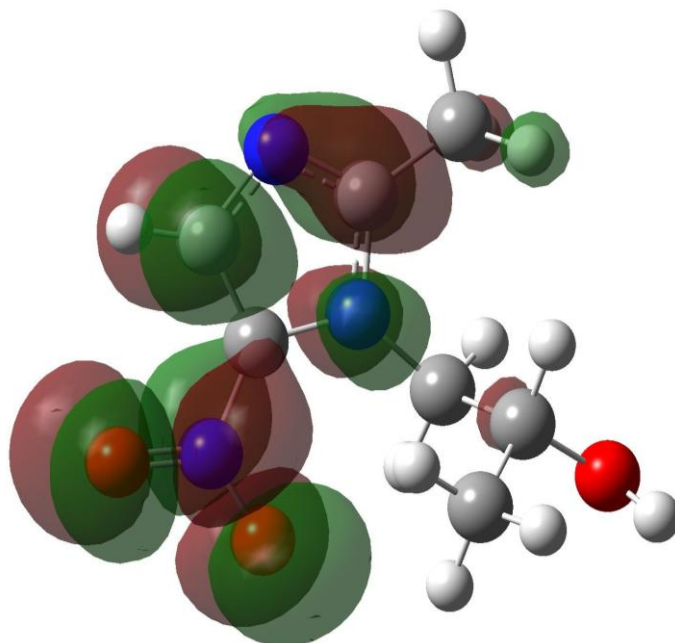


**Figure 17.** The lowest unoccupied molecular orbital (LUMO) density of Secnidazole (SEC) using DFT at the B3LYP/6-31G\* basis set level.

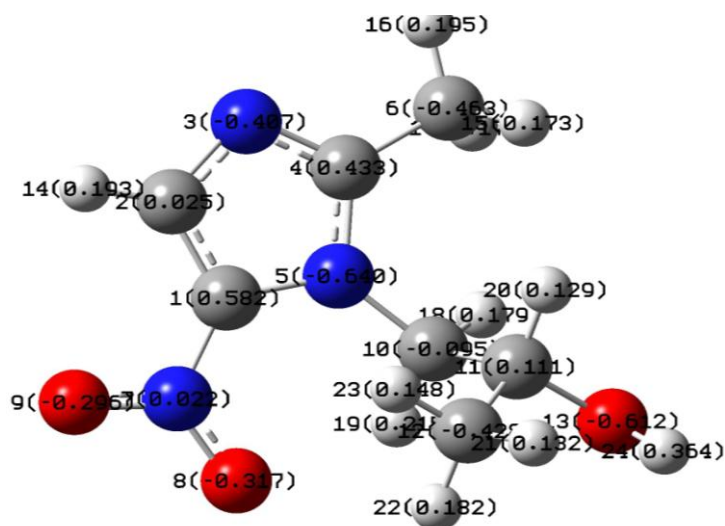


**Figure 18.** Mulliken charges population analysis of Secnidazole (SEC) using DFT at the B3LYP/6-31G\* basis set level.

According to frontier orbital theory, the reaction of reactants mainly occurred on the highest occupied molecular orbital (HOMO) and lowest unoccupied molecular orbital (LUMO). So it was imperative to investigate the distribution of HOMO and LUMO for exploration of inhibition mechanism. From Figs. 15 and 16, it could be seen that SEC have similar HOMO and LUMO distributions, which were all located on imidazole ring. This kind of distribution favoured the preferential adsorption of imidazole ring on metal surface in two ways: one was that the unoccupied d

orbitals of Fe atom accepted electrons from inhibitor molecule to form coordinate bond. The other was that the inhibitor molecule accepted electrons from Fe atom with its anti-bonding orbitals to form back-donating bond.

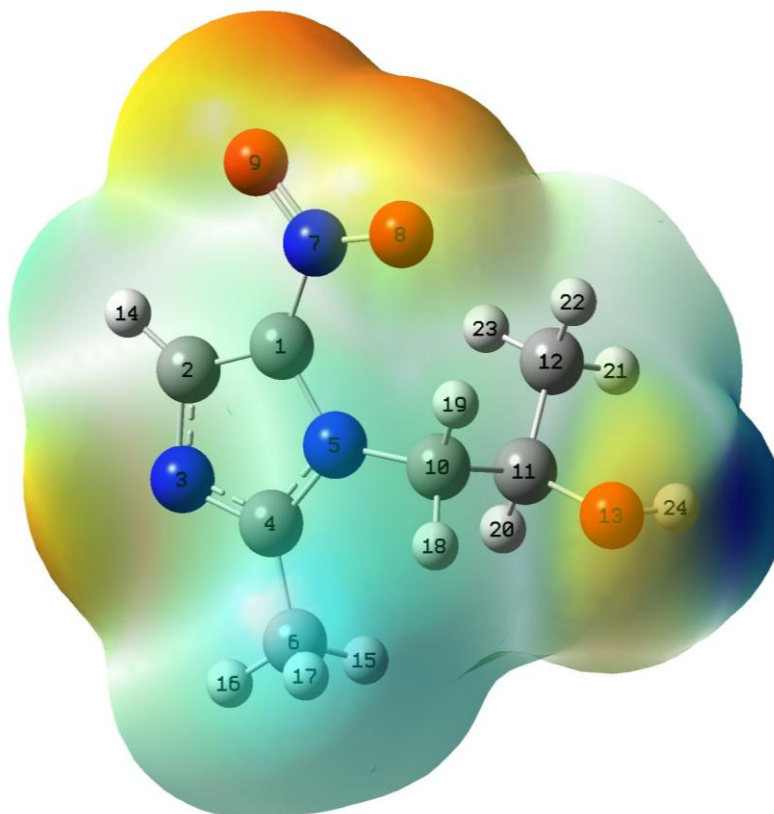


**Figure 19.** Total electron density diagram of Secnidazole (SEC) – [the electron rich region is red and the electron poor region is blue for the SEC neutral molecule].

It has been reported that the more negative the atomic charge of the adsorbed centre, the more easily the atom donates its electrons to the unoccupied orbital of metal [6, 7]. Fig. 18 shows the Mulliken charges of the atoms in SEC molecule. By careful inspection of the values of Mulliken charges, the largest negative atom is found on the N5 of the imidazole ring.

Other atoms with excess negative charges include N3 of the imidazole ring, O8 and O9 of the -NO<sub>2</sub> group as well as O13 of the -OH group. This is further supported by Fig. 19, where the total electron density is located around these atoms. Thus, the adsorption of SEC on mild steel would take place through the imidazole heterocyclic ring, the nitro and hydroxyl functional groups. The simultaneous adsorption of the three functional groups forces the inhibitor molecule to be horizontally oriented at the metal surface.

From Table 4, the negative total energy indicates that SEC is a very stable molecule and is less prone to be split or broken apart. The dipole moment of SEC is 4.97 Debye (D) ( $16.576 \times 10^{-30}$  Cm), which is higher than that of H<sub>2</sub>O ( $\mu = 6.23 \times 10^{-30}$  Cm).

**Table 4.** Optimized DFT parameters at the B3LYP/6-31G\* level for SECNIDAZOLE (SEC)

Total energy (a.u)	-662.965
E <sub>HOMO</sub> (eV)	-0.267
E <sub>LUMO</sub> (eV)	-0.107
ΔE (E <sub>LUMO</sub> - E <sub>HOMO</sub> )(eV)	0.159
Dipole moment(D)	4.971
Molecular weight (amu)	185.182
Electronic energy(eV)	-13948.723
Ionization potential (eV)	10.162
Cosmo Area (Å <sup>2</sup> )	198.532
Cosmo Volume (Å <sup>3</sup> )	210.20
Core-Core repulsion(eV)	11319.00

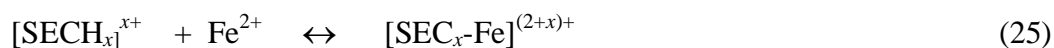
The high value of dipole moment probably increases the adsorption between chemical compound and metal surface [87]. Accordingly, the adsorption of SEC molecules from the aqueous solution can be regarded as a quasi-substitution process between the SEC compound in the aqueous phase [SEC<sub>(sol)</sub>] and water molecules at the electrode surface [H<sub>2</sub>O<sub>(ads)</sub>]. Moreover, a smaller energy gap, ΔE (E<sub>LUMO</sub>-E<sub>HOMO</sub>) of 0.159 (eV), a higher molecular weight, higher area and volume enhances effective adsorption of SEC on the mild steel surface thus decreasing the corrosion rate of the mild steel.

### 3.9. Mechanism of inhibition action of SEC on mild steel

From the experimental and theoretical results obtained, the inhibition effect of SEC in H<sub>2</sub>SO<sub>4</sub> solution can be explained as follows:



Thus, in aqueous acidic solutions, the SEC exists either as neutral molecules or in the form of cations (protonated SEC). Generally, two modes of adsorption could be considered. The neutral SEC may be adsorbed on the metal surface via the chemisorption mechanism involving the displacement of water molecules from the metal surface and the sharing of electrons between nitrogen, oxygen atoms and iron. The SEC molecules can be adsorbed also on the metal surface on the basis of donor-acceptor interactions between π-electrons of the heterocycle and vacant d-orbitals of iron. On the other hand, SO<sub>4</sub><sup>2-</sup> could adsorb on the metal surface [88], then the protonated SEC may adsorb through electrostatic interactions between the positively charged molecules and already adsorbed sulphate ions. Thus, the metal complexes of Fe<sup>2+</sup> and SEC or protonated SEC might be formed as follows:



These complexes might adsorb onto steel surface by van der Waals force to form a protective film to keep the mild steel surface from corrosion. Similar mechanism has been documented by us [15] and others [49].

#### 4. CONCLUSIONS

The following conclusions may be drawn from the study:

1. Secnidazole (SEC) acts as a good inhibitor for the corrosion of mild steel in 0.01 M H<sub>2</sub>SO<sub>4</sub>. Inhibition efficiency values increase with the inhibitor concentration but decrease with the acid concentration and the temperature.
2. The rate constant ( $k$ ) decreases obviously after adding SEC in 0.01-0.04 M H<sub>2</sub>SO<sub>4</sub> solution, while the reaction constant ( $B$ ) increases. The value of both apparent activation energy ( $E_a$ ) and Arrhenius pre-exponential factor ( $A$ ) also increase after SEC addition in 0.01 M H<sub>2</sub>SO<sub>4</sub>.
3. The adsorption of SEC on steel surface was found to obey with Langmuir adsorption isotherm. The adsorption process is spontaneous, exothermic and accompanied with a decrease in entropy of the system from thermodynamic point of view.
4. Quantum chemical calculations using DFT reveal that the adsorption of SEC on mild steel would take place through the imidazole heterocyclic ring, the nitro and hydroxyl functional groups. The simultaneous adsorption of the three functional groups forces the inhibitor molecule to be horizontally oriented at the metal surface.
5. The introduction of SEC into 0.01 M H<sub>2</sub>SO<sub>4</sub> solution results in the formation of a protective film on the mild steel surface, which may contain the complex of SEC-Fe<sup>2+</sup>, and effectively protects steel from corrosion.

#### References

1. M. Benabdellah, K.F. Khaled, B. Hammouti, *Mater. Chem. Phys.* 120 (2010) 61.
2. A.R. Afidah, J. Kassim. *Recent Patents on Mater. Sci.* 1 (2008) 223.
3. I.B. Obot, N.O. Obi-Egbedi, N.W. Odozi, *Corros. Sci.* 52 (2010) 923.
4. I.B. Obot, N.O. Obi-Egbedi, *Corros. Sci.* 52 (2010) 282.
5. I.B. Obot, N.O. Obi-Egbedi, *Surf. Rev. Lett.* 15(6) (2008) 903.
6. I.B. Obot, N.O. Obi-Egbedi, *Mater. Chem. Phys.* 122(2-3)(2010)325.
7. I.B. Obot, N.O. Obi-Egbedi, *Corros. Sci.* 51 (2009) 276.
8. S.A. Umoren, I.B. Obot, E.E. Ebenso, N. O. Obi-Egbedi, *Int. J. Electrochem. Sci.* 3(2008) 1029.
9. E.E. Ebenso, H. Alemu, S.A. Umoren, I.B.Obot, *Int. J. Electrochem. Sci.* 4 (2008) 1325.
10. E.E. Ebenso, T. Arslan, F. Kandemirli, N. Caner, I. Love, *Int. J. Quant. Chem.* 110 (2010) 1003.
11. P.B. Raja, M.G. Sethuraman, *Mater. Lett.* 62 (2008) 113.
12. X. Li, S. Deng, H. Fu, *Prog. Org. Coat.* 67 (2010) 420.
13. I.B. Obot, N.O. Obi-Egbedi, *Colloids and Surfaces A: Physicochem.Eng. Aspects.* 330 (2008) 207.
14. I.B. Obot, N.O. Obi-Egbedi, S.A. Umoren, *Int. J. Electrochem. Sci.* 4 (2009) 863.
15. I.B. Obot, N.O. Obi-Egbedi, *Corros. Sci.* 52 (2010) 198.
16. I.B. Obot, N.O. Obi-Egbedi, S.A. Umoren, *Corros. Sci.* 51 (2009) 1869.
17. I.B.Obot, *Portugaliae Electrochimica Acta.* 2795) (2009) 539.

18. E.E. Ebenso, N.O. Eddy, A.O. Odiongeyi, *Port. Electrochimica Acta* 27(1) (2009) 13.
19. T. Arslan, F. Kandemirli, E.E. Ebenso, I. Love, H. Alemu, *Corros. Sci.* 51 (2009) 35.
20. N.O. Eddy, U.J. Ibok, E.E. Ebenso, A. El Nemr, E.S.H. El Ashry, *J. Mol. Mod.* 15 (2009) 1085.
21. N.O. Eddy, E.E. Ebenso, U. J. Ibok, *J. Appl. Electrochem.* 40(2) (2010) 445.
22. N.O. Eddy, S.A. Odoemelam, P. Ekwumengbo, *Sci. Res. Essays* 4(1) (2009) 33.
23. N.O. Eddy, S.A. Odoemelam, A.J. Mbaba, *Afri. J. Pure & Appl. Chem* 2(12) (2008) 132.
24. N.O. Eddy, S. R. Stoyanov, E.E. Ebenso, *Int. J. Electrochem. Sci.* 5 (2010) 1127.
25. N.O. Eddy, E.E. Ebenso, *Int. J. Electrochem. Sci.* 5 (2010) 731.
26. R. Solmaz, G. Kardas, B. Yazici, M. Erbil, *Protection of Metals* 41(6) (2005) 581
27. S.K. Shukla, A.K. Singh, I. Ahmed, M.A. Quraishi, *Mater. Lett.* 63 (2009) 819.
28. M. Abdallah, *Corros. Sci.* 44 (2002) 728.
29. M. Abdallah, *Corros. Sci.* 46 (2004) 1996.
30. M. M. El-Naggar, *Corros. Sci.* 49 (2007) 2226.
31. S.K. Shukla, M.A. Quraishi, *Corros. Sci.* 51 (2009) 1007.
32. A.K. Singh, M.A. Quraishi, *Corros. Sci.* 52 (2010) 152.
33. E.E.F. Elsherbini, *Mater. Chem. Phys.* 60 (1999) 286.
34. M.S. Morad, *Corros. Sci.* 50 (2008) 436.
35. S.K. Shukla, M.A. Quraishi, *J. Appl. Electrochem.* 39(9) (2009) 1517.
36. R.A. Prabhu, A.V. Shanbhag, T.V. Venkatesha, *J. Appl. Electrochem.* 37 (2007) 491.
37. P. XueHui, G. Wenjaun, I. WeiHui, X. JianDong, H. BaoRong, *Sci. Chin. Ser. B: Chem.* 51 (2008) 928.
38. I. Ahamad, M.A. Quraishi, *Corros. Sci.* 52 (2010) 651.
39. N. Girginkardesler, C. Balcioglu, O.K. Ertan, *European Society of Clinical Microbiology and Infectious Diseases* 9(2) (2003) 110.
40. S.A. Umoren, M.M. Solomon, I.I. Udoso, A.P. Udoh, *Cellulose* 17(3) (2010) 635.
41. M.M. Solomon, S.A. Umoren, I.I. Udoso, A.P. Udoh, *Corros. Sci.* 52(4) (2010), 1317.
42. S.A. Umoren, I.B. Obot, E.E. Ebenso, N.O. Obi-Egbedi, *Desalination.* 247 (2009) 561.
43. S.A. Umoren, I.B. Obot, N.O. Obi-Egbedi, *J. Mater. Sci.* 44 (2009) 274.
44. A.Y. Musa, A.A. Khadom, A. H. Kadhum, A.B. Mohamad, M.S. Takriff, *J. Taiwan Ins. Chem. Engr.* 41 (2010) 126.
45. A.A. Khadom, A.S. Yaro, A. H. Kadum, *J. Taiwan Ins. Chem. Engr.* 41 (2010) 122.
46. M. Bouklah, B. Hammouti, M. Lagrenee, F. Bentiss, *Corros. Sci.* 48 (2006) 2831.
47. A.D. Mercer, *Br. Corros J.* 20(2) (1985) 61.
48. J.O.M. Bockris, D. Drazic, *Electrochimica Acta* 7 (1962) 29B.
49. H. Ashassi-Sorkhabi, S.A. Nabavi-Amri, *Acta Chim. Slov.* 47 (2000) 512.
50. X. Li, S. Deng, H. Fu, G. Mu, *Corros. Sci.* 51 (2009) 620.
51. T.P. Zhao, G.N. Mu, *Corros. Sci.* 41 (1999) 1937.
52. A.K. Maayta, N.A.F. Al-Rawashdeh, *Corros. Sci.* 46 (2004) 1129.
53. Y. Abboud, A. Abourriche, T. Saffaj, M. Berrada, M. Charrouf, A. Bennamara, H. Hannache, *Desalination.* 237 (2009) 175.
54. P.B. Mathur, T. Vasudevan, *Corrosion* 38 (1982) 171.
55. I. Wang, *Corros. Sci.* 48 (2006) 608.
56. M.A. Quraishi, H.K. Sharma, *Mater. Chem. Phys.* 78 (2002) 18.
57. E.E. Oguzie, G.N. Onuoha, *Mater. Chem. Phys.* 89 (2005) 305.
58. S.A. Umoren, I.B. Obot, E.E. Ebenso, P.C. Okafor, O. Ogbobe, E.E. Oguzie, *Anti-Corros. Meth. Mater.* 53 (5) (2006) 277.
59. S.A. Umoren, I.B. Obot, *Surf. Rev. Lett.* 15(3) (2008) 277.
60. A.R.S. Priya, V.S. Muralidharam, A. Subramania, *Corrosion* 64 (2008) 541.
61. E.E. Ebenso, *Mater. Chem. Phys.* 79 (2003) 58.
62. E.A. Noor, A.H. Al-Moubaraki, *Mater. Chem. Phys.* 110 (2008) 145.

63. F. Bentiss, M. Bouanis, B. Mernari, M. Traisnel, H. Vezin, M. Lagrenee, *Appl. Surf. Sci.* 253 (2007) 3696.
64. A.K. Singh, M.A. Quraishi, *Corros. Sci.* 52(2) (2009) 651.
65. Z. Tao, S. Zhang, W. Li, B. Hou, *Corros. Sci.* 51 (2009) 2588.
66. E.E. Oguzie, V.O. Njoku, C.K. Enenebeaku, C.O. Akalezi, C. Obi, *Corros. Sci.* 50 (2008) 3480.
67. E.A. Noor, *J. Appl. Electrochem.* 39 (2009) 1465.
68. M.A. Amin, Q. Mohsen, O.A. Hazzazi, *Mater. Chem. Phys.* 114 (2009) 908.
69. M.A. Amin, S.S. Abd El Rehim, M.M. El-Naggar, H.T.M. Abdel-Fatah, *J. Mater. Sci.* 44 (2009) 6258
70. M.A. Migahed, H.M. Mohammed, A.M. Al-Sabagh, *Mater. Chem. Phys.* 80 (2003) 169.
71. A.A. Abdul Azim, L.A. Shalaby, H. Abbas, *Corros. Sci.* 14 (1974) 21.
72. I.Tang, X. Li, I. Lin, G. Mu, G. Liu, *Mater. Chem. Phys.* 97 (2006) 301.
73. Z. Sibel, P. Dogan, B. Yazici, *Corros. Rev.* 23 (2005) 217.
74. G. Moretti, F. Guidi, G. Grion, *Corros. Sci.* 46 (2004) 387.
75. A.Y. Musa, A.A.H. Kadhum, A.B. Mohamad, A.R. Daud, M.S. Takriff, S.K. Kamarudin, *Corros. Sci.* 51 (2009) 2399.
76. E.A. Noor, *Int. J. Electrochem. Sci.* 2 (2007) 996.
77. M. Benabdellah, A. Aouniti, A. Dafali, B. Hammouti, M. Benkaddour, A. Yahyi, A. Ettouhami, *Appl. Surf. Sci.* 252 (2006) 8341.
78. A.M. Badiea, K.N. Mohana, *Corros. Sci.* 51 (2009) 2231.
79. S. Martinez, I. Stern, *Appl. Surf. Sci.* 199 (2002) 83.
80. I.Tang, G. Mu, G. Liu, *Corros. Sci.* 45 (2003) 2251.
81. X. Li, G. Mu, *Appl. Surf. Sci.* 252 (2005) 1254.
82. G. Mu, X. Li, G. Liu, *Corros. Sci.* 47 (2005) 1932.
83. J.M. Thomas, W.J. Thomas, *Introduction to the principles of Heterogeneous Catalysis*, Fifth ed., Academic Press, London, 1981, p. 14.
84. N. Khalil, *Electrochim. Acta* 48 (2003) 2635.
85. G. Gao, C. Liang, *Electrochim. Acta* 52 (2007) 4554.
86. C. Adamo, V. Barone, *Chem. Phys. Lett.* 330 (2000) 152.
87. S. Vijayakumar, P. Kolandaivel, *J. Mol. Struct. (THEOCHEM)* 770 (2006) 23.
88. K. Ramji, D.R. Cairns, S. Rajeswari, *Appl. Surf. Sci.* 254 (2008) 4483.
89. F. Bentiss, M. Traisnel, M. Lagrenee, *Corros. Sci.* 42 (2000) 127.